World Academy of Science, Engineering and Technology
International Journal of Aerospace and Mechanical Engineering
Vol:15, No:3, 2021

The Use of the Flat Field Panel for the On-Ground Calibration of Metis Coronagraph on Board of Solar Orbiter

C. Casini, V. Da Deppo, P. Zuppella, P. Chioetto, A. Slemer, F. Frassetto, M. Romoli, F. Landini, M. Pancrazzi, V. Andretta, E. Antonucci, A. Bemporad, M. Casti, Y. De Leo, M. Fabi, S. Fineschi, F. Frassati, C. Grimani, G. Jerse, P. Heinzel, K. Heerlein, A. Liberatore, E. Magli, G. Naletto, G. Nicolini, M.G. Pelizzo, P. Romano, C. Sasso, D. Spadaro, M. Stangalini, T. Straus, R. Susino, L. Teriaca, M. Uslenghi, A. Volpicelli

***Abstract*—**Solar Orbiter, launched on February 9th 2020, is an ESA/NASA mission conceived to study the Sun. The payload is composed of 10 instruments, among which there is the Metis coronagraph. A coronagraph aims at taking images of the solar corona: the occulter element simulates a total solar eclipse. This work presents some of the results obtained in the visible light band (580-640 nm) using a flat field panel source. The flat field panel gives a uniform illumination; consequently, it has been used during the on-ground calibration for several purposes: evaluating the response of each pixel of the detector (linearity); and characterizing the Field of View of the coronagraph. As a conclusion, a major result is the verification that the requirement for the Field of View (FoV) of Metis is fulfilled. Some investigations are in progress in order to verify that the performance measured on-ground did not change after launch.

***Keywords*—**Space instrumentation, Metis, solar coronagraph, flat field.

I. Introduction

THE study of the Sun and its surroundings has continuously known major breakthrough since the invention of the coronagraph by Bernard Lyot in the 1930s [1], enabling to study the solar corona not only during solar eclipses. Indeed, the brightness ratio between the solar disk and the corona is, depending on the radial distance, close to 10^8. Besides, Lyot took in consideration atmospheric turbulences and built the first coronagraph in altitude, on the Pic du Midi (France, 2810 m) to reduce their signal contribution. The spatial conquest during the following of the twentieth century offered a way to circumvent this issue. Several coronagraphs have been therefore embedded to study the solar corona. A total solar eclipse is simulated by means of an occulter that blocks the photosphere (i.e. the visible solar disk).

The last missions are the ones concerning: SOHO (with the coronagraph C1-LASCO/C2 and C3) [2]-[4]; STEREO with SECCHI instruments composed by 5 telescopes that include two coronagraphs COR1 and COR2 [5], [6]; the suborbital mission HERSCHEL with the HECOR and SCORE coronagraphs [7], [8]; the Parker Solar Probe mission with the WIRSP coronagraph. These orbital coronagraphs are still working to study the coronal activity survey, the physics of Coronal Mass Ejections (CMEs), the electron density evolution [4], [5] but there are still some open questions. The Solar Orbiter mission, which spacecraft was launched on February 2020, is the first one reaching the inner heliosphere, and aiming to observe the Sun from elliptical orbits with perihelion and aphelion distances as small as 0.28 AU and of about 0.8 AU; and simultaneously going out of the ecliptic plane.

Solar Orbiter payload is composed of 10 instruments, among which Metis, the coronagraph, it is created to answer to the major open issues in understanding the corona and the solar wind, and concerning: the origin and acceleration of the solar wind streams; the origin, acceleration and transport of the solar energetic particles (SEPs); and the transient ejection of coronal mass and its evolution in the inner heliosphere (CMEs). In addition, Metis can contribute to the study of Sungrazing comets [9]. To answer these questions, the instrument needs to be calibrated on-ground and during the first phase of the mission. For the on-ground calibration, a flat field panel is used to simulate the solar uniform luminosity.

This article presents the development of the on ground calibration of Metis's flat field panel in the visible light (580-640 nm), for which resulting data were used to determine the performance of the instrument and its radiometric efficiency.

The flat field panel is used during the on ground calibration for several purposes: evaluating the response of each pixel of the detector; and characterizing the FoV of the coronagraph.

II. Description of the Metis Coronagraph

Metis is an aplanatic Gregorian telescope; it has an inverse external occulter to block the light of the solar disk. This novelty is used to reduce the extremely high thermal load on the instrument at the spacecraft perihelion. In the following the scheme and the optical path inside the instrument are described.

A. Optical Layout

In Fig. 1, a CAD transparent picture is presented to show the components of Metis that help to describe the optical path.

All the sunlight enters from the inverted external occulter (IEO), the light from the solar disk is rejected to the aperture from M_0. There is a boom that consists of an opaque tube

Chiara Casini is with CNR-IFN-Padova, Italy (e-mail: chiara.casini@pd.ifn.cnr.it).

bounded at its ends by IEO and M_0 and containing the Shield Entrance Aperture (SEA) diaphragm, which aims to reduce the diffused light inside the tube.

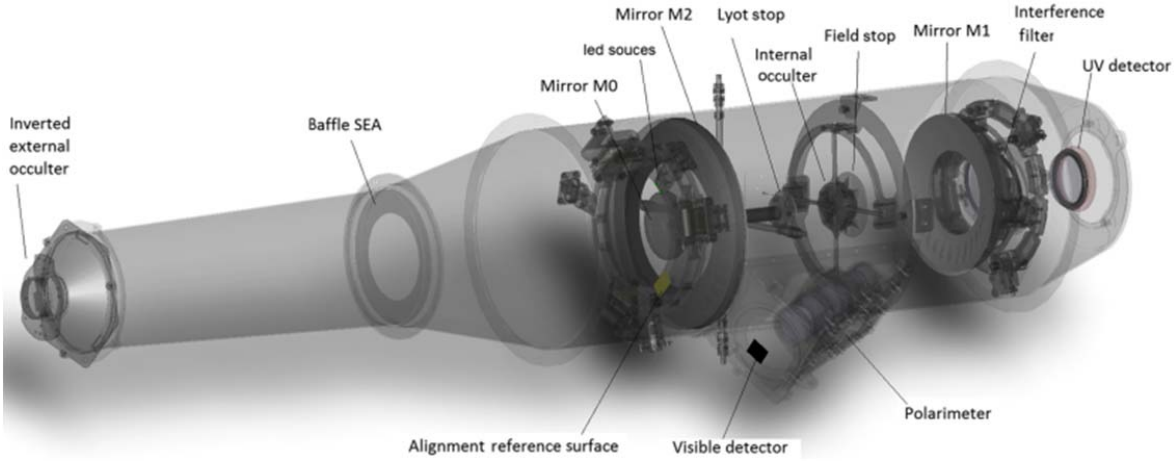

Fig. 1 Metis 3D CAD with the principal elements of Metis

The corona signal is reflected by the mirror M_1, passes the Field Stop (FS), Internal Occulter (IO) and Lyot Stop (LS) as drawn in Fig. 2. Also the light from the solar disk that is back rejected by M0 is shown. To help the reader understand the picture here follows the list of acronyms used. IEO: inverted external occulter; M_0, M_1 and M_2 are the mirrors along the Metis optical path; LS: Lyot Stop; IO: Internal Occulter; FS: Field Stop; IF: Interference Filter.

Mirror M_1 creates real images of the edges of IEO and M_0 which are the main sources of the diffused light. The image of the edges of the IEO is locked to the IO, while the image (generated by M_1) of the edges of the mirror M_0 is eliminated by the LS. Then, the coronal light arrives at the mirror M_2 and it is reflected in the direction of the dichroic beam-splitter, IF. The interference filter is optimized for narrowband spectral transmission in the ultraviolet (UV, 121.6 nm, HI Lyman-α) and broadband spectral reflection in the visible (VIS, 580–640 nm) spectral ranges.

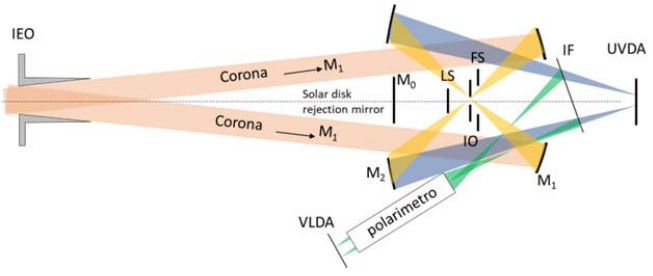

Fig. 2 Schematic views of Metis coronagraph in both UV channel and Visible Light channel

The UV light arrives on the UVDA (UV Detector Assembly), described in Subsection *B*. The visible light is reflected and enters in a polarimetric unit to perform measurements of the polarization of the coronal radiation. This coronal light passes through a sequence of an optical collimating system (CD collimating), a bandpass filter (BP), a linear polarization analyzer and is focused channel detector (Visible Channel Detector Assembly, VLDA) passing in optical system focusing on the plane of the visible. The polarization analyzer consists of a quarter-wave delay foil (QWP), a delay foil variable, liquid crystal (LCVR, liquid crystals variable retarder - Electro-optical Polarization Module Package, PMP), a linear polarizer (LP).

B. Ultraviolet (UV) and Visible (VL) Detection

In this section the detectors on board Metis are described. The UV detector (UVDA) was developed by CMOSIS[1] and MPS[2] specifically for the Solar Orbiter mission located at the focal plane of the UV channel, an Intensified and Active Pixel Sensor (IAPS). It consists in a Micro Channel Plate (MCP), with a K-Br photocathode and is optically coupled, via an optical fiber cone, to an APS (Active Pixel Sensor): 1024 x 1024 sensor. The cone resizes the image of the focal plane of the detector so that it fits the sensor dimensions. Scaling is 2:1, so the 15 micrometer pixel size results in an effective 30 micrometer focal plane sampling element. The detector allows up to 10 readings per second. The incoming UV photons extract electrons from the photocathode, which are collected and amplified by the MCP, producing an electron cloud for each single photon incident on the intensifier. The electrons are then accelerated towards an aluminum (Al) screen placed at a voltage of a few kV to impact on a phosphor which converts them back into photons.

The detector can operate in Analog mode or in Photon Counting Mode depending on the gain of the intensifier. In analog (or integration) mode, the UVDA collects the charge created by the incoming photons during the entire set integration time. In photon counting mode, the UVDA intensifier is operated at such a gain that each single photon hitting the photocathode produces a signal on the APS. The APS will be read at the maximum speed of 10 frames/s which

[1] http://www.cmosis.com/
[2] Max-Planck-Institut fur Sonnensystemforschung, Gottingen, Germany

is enough to have no more than one photon hitting a single pixel per frame read. The position of the single photon is identified through the centroid of the light distribution, and its coordinates are transmitted by telemetry.

As for the visible light, the VLDA detector consists of a camera sensitive to the spectral range 580-640 nm. It is a complementary metal-oxide semiconductor (APS CMOS) also specifically developed by CMOSIS and MPS for the Solar Orbiter mission. The same detector is also used for the PHI instrument, other instrument aboard Solar Orbiter. The VLDA includes an APS detector with a sensor of 2048 x 2048 pixels that are 10 µm long. Although the detector allows a reading of 10 frames per second, it is operated at a lower frequency, with minimum integration times of 1 second.

The VLDA collects the charge created by the incoming photons during the whole set integration time and, like the UVDA, the data are transmitted at the telemetry.

III. Ground Calibration Methods and Results

A coronagraph needs on ground calibration and therefore a setup that simulates the sunlight. The latter is performed with a flat field panel, enabling a uniform illumination. This permits to calibrate the Metis detectors, consisting in CCD pixel arrays for the visible and UV light. The obtained calibration images are referred hereafter as flat field images. This section is dedicated to the description of the experimental setup, and to the preliminary calibration work on the flat field images.

A. Optical Layout of the Laboratory Calibration Test Set-Up

To measure the irradiance we use the model Spike-a flat field. This flat field panel is composed by a LED matrix with several layers of diffusing material to obtain a quasi-uniform illumination (at 99%). Indeed, the brightness is higher for central solid angles with respect to the border. To solve this problem a 9V-powered flat field panel was put in the center of the aperture of Metis and perpendicular to the optical axis of the telescope. This voltage value is critical since lower voltage can induce temporal fluctuation of the luminosity.

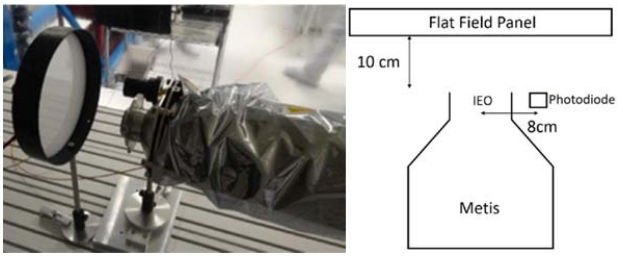

(a) (b)

Fig. 3 (a) Optical layout of Metis in the laboratory calibration test set-up. (b) Diagram of the top and sectional view of the flat field panel, of the photodiode and of Metis with relative distances

A picture of the experimental setup is presented in Fig. 3 (a), and the experimental scheme in Fig. 3 (b). The flat field panel was positioned 10 cm from the Metis aperture, and a photodiode is set 8 cm from the center of the IEO to check the flat field panel illumination performances.

The photodiode (model AXUV100G) measures the irradiance of the flat field panel, with an internal quantum efficiency of 100%. As represented in Fig. 4, in front of the photodiode there is a bandpass filter, provided by the OPTEC (Optical and Optoelectronic systems). The filter (10 mm x 10 mm) is optimized for the visible wavelength: 580nm-640 nm. The responsivity provides us a quantitative indication of how much current is generated from each Watt of incident power. One of the images produced out of this configuration is shown in Fig. 5.

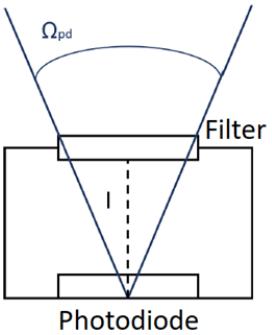

Fig. 4 Scheme of the photodiode and filter

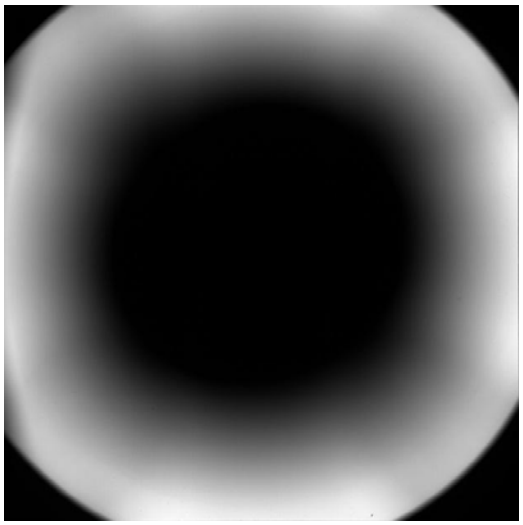

Fig. 5 Image of the flat field panel after the subtraction of the dark

The image was acquired in a series of four frames, with different times of exposure. The next sub-section is dedicated to the studies implying those images, such as the study of the centroid determination (B).

B. Centroid Determination of the Flat Field Image

The used method for the centroid determination is based on the plot profiles along the rows and columns. The results obtained for the analyzed images are equivalent. We report therefore only those of the FF image from which the dark has already been subtracted.

Since the aim is to find the center of the image, we reduced our study to the range of columns from 800 to 1400 (similar to that used for a row) because we have the dark areas at the edges, caused by the front stop (FS). For each column, we created the profile, such as the one in Fig. 6.

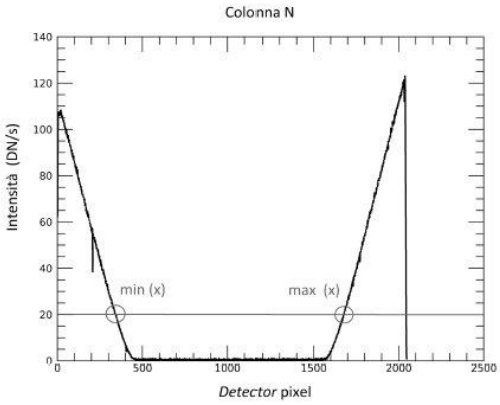

Fig. 6 Description of the plot method applied on the averaged profile of column

To find the mean value, we draw the horizontal line of intensity = 20 DN/s, chosen arbitrarily in an area of the profile with a higher gradient free from background noise. Intersections with the profile define the values min (x) and max (x). The average value of a column (or a row) is defined from min (x) and max (x) through (1):

$$Average = \frac{\min(x)+\max(x)}{2} \quad (1)$$

This procedure was used for each column and each row. To eliminate errors due to noise fluctuations along the profile, we performed a smoothing procedure, averaging the value of our pixel with the values of the 3 previous and 3 subsequent pixels.

The displacement of the center could depend on the correction to the inclination of the interference filter (IF) during the integration and alignment phase. This deviation is due to the imperfect positioning of the IF, whose rejection determines a misalignment between the optical and effective axis and the optical axis of the polarimeter and a deformation of the vignetting. By averaging on all profiles in the interval [800; 1400], the average value for x and y are x = 1013 ± 8 and y = 1089 ± 9.

IV. Conclusion

On ground calibrations are fundamental, in particular that with the flat field panel. The determination of the center of the image has crucial importance: some Metis optical components could have moved during its launch. Consequently, "investigations" are in progress in order to verify that this did not broadly impact the optical performances of the coronagraph.

Comparing the on ground calibration and in flight calibrations gives, also, the opportunity to know the degradation of the system and to correct, from time to time and as possible, this effect.

Acknowledgment

The Metis programme is supported by the Italian Space Agency (ASI) under the contracts to the co-financing National Institute of Astrophysics (INAF): Accordi ASI-INAF N. I-043-10-0 and Addendum N. I-013-12-0/1, Accordo ASI-INAF N. 2018-30-HH.0 and under the contracts to the industrial partners: ASI-TASI N. I-037-11-0 and ASI-ATI N. 2013-057-I.0. The Metis team thanks Barbara Negri, Enrico Flamini, Marco Castronuovo of the Italian Space Agency and Roberto Della Ceca, Giuseppe Malaguti of the Istituto Nazionale di Astrofisica for their continuous support during the development of the coronagraph. A special thanks to Filippo Marliani of the European Space Agency for his dedication to the program and his high standard of excellence. The testing of Metis was performed by an industrial consortium constituted by OHB Italia S.p.A. (acting as Prime Contractor towards ASI), Thales Alenia Space Italia S.p.A. (Co-Prime Contractor with the specific responsibility of the instrument AIT). ALTEC has provided logistics and technical support for the INAF Optical Payload Systems. The primary and secondary mirrors were provided as Czech contribution to Metis; the mirror hardware development was possible thanks to the Czech PRODEX Programme. The UVDA assembly was provided as a German contribution to Metis, thanks to the financial support of DLR (grant 50 OT 1201). The VLDA assembly was provided under Contract 2013- 058-I.0 with the Italian Space Agency (ASI).

References

[1] Lyot, B. (1939). The study of the solar corona and prominences without eclipses (George Darwin Lecture, 1939). on. Not. Royal Astron. Soc., 99, 580–594.

[2] Moran, T. G.; Davila, J. M.; Morrill, J. S.; Wang, D.; Howard, R. Solar and Heliospheric Observatory/Large Angle Spectrometric Coronagraph Polarimetric Calibration. *Sol Phys* 2006, *237* (1), 211–222. https://doi.org/10.1007/s11207-006-0147-9.

[3] Morrill, J. S.; Korendyke, C. M.; Brueckner, G. E.; Giovane, F.; Howard, R. A.; Koomen, M.; Moses, D.; Plunkett, S. P.; Vourlidas, A.; Esfandiari, E.; Rich, N.; Wang, D.; Thernisien, A. F.; Lamy, P.; Llebaria, A.; Biesecker, D.; Michels, D.; Gong, Q.; Andrews, M. Calibration of the Soho/Lasco C3 White Light Coronagraph. *Sol Phys* 2006, *233* (2), 331–372. https://doi.org/10.1007/s11207-006-2058-1.

[4] Llebaria, A.; Lamy, P. L.; Bout, M. V. Lessons Learned from the SOHO/LASCO-C2 Calibration; Fineschi, S., Gummin, M. A., Eds.; San Diego, California, USA, 2004; p 26. https://doi.org/10.1117/12.506159.

[5] Howard, R. A.; Moses, J. D.; Vourlidas, A.; Newmark, J. S.; Socker, D. S.; Plunkett, S. P.; Korendyke, C. M.; Hurley, A.; Davila, J. M.; Thompson, W. T.; Cyr, O. C. S.; Mentzell, E.; Mehalick, K.; Lemen, J. R.; Wuelser, J. P.; Duncan, D. W.; Tarbell, T. D.; Harrison, R. A.; Waltham, N. R.; Lang, J.; Davis, C. J.; Laboratory, R. A.; Eyles, C. J.; Halain, J. P.; Defise, J. M.; Mazy, E.; Rochus, P.; Ravet, M. F.; Delmotte, F.; Auchere, F.; Delaboudiniere, J. P.; Bothmer, V. Sun Earth Connection Coronal and Heliospheric Investigation. 56.

[6] Thompson, W. T.; Davila, J. M.; Fisher, R. R.; Orwig, L. E.; Mentzell, J. E.; Hetherington, S. E.; Derro, R. J.; Federline, R. E.; Clark, D. C.; Chen, P. T.; Tveekrem, J. L.; Martino, A. J.; Novello, J.; Wesenberg, R. P.; StCyr, O. C.; Reginald, N. L.; Howard, R. A.; Mehalick, K. I.; Hersh, M. J.; Newman, M. D.; Thomas, D. L.; Card, G.; Elmore, D. The COR1 Inner Coronagraph for STEREO-SECCHI. 11.

[7] Auchère, F.; Ravet-Krill, M.-F.; Moses, J. D.; Rouesnel, F.; Barbet, D.; Hecquet, C.; Jérome, A.; Mercier, R.; Delmotte, F.; Newmark, J. S.

HECOR, a HElium CORonagraph Aboard the Herschel Sounding Rocket. 11.

[8] Pancrazzi, M.; Focardi, M.; Landini, F.; Romoli, M.; Fineschi, S.; Gherardi, A.; Massone, G.; Pace, E.; Paganini, D.; Rossi, G. SCORE CCD Visible Camera Calibration for the HERSCHEL Suborbital Mission; Fineschi, S., Fennelly, J. A., Eds.; San Diego, CA, 2009; p 74380J. https://doi.org/10.1117/12.831267.

[9] Antonucci, E. Metis Scientific Performance Report. 2017, No. 4, 36.